

IMECE2006-13763

THE PERFORMANCE OF AN ENTHALPY RECOVERY WHEEL IN VENTILATION OF CMU'S IW

Chaoqin Zhai
School of Architecture
Carnegie Mellon University
5000 Forbes Ave
Pittsburgh, PA 15213
chaoqin@cmu.edu

David H. Archer
Department of Mechanical Engineering
Carnegie Mellon University
5000 Forbes Ave
Pittsburgh, PA 15213
archerdh@andrew.cmu.edu

John C. Fischer
SEMCO Incorporated
1800 East Pointe Drive
Columbia, MO 65201
johnfischer@bellsouth.net

ABSTRACT

The operating performance of an enthalpy recovery wheel exchanging heat and moisture between outside and exhaust air streams in the ventilation system of Carnegie Mellon University (CMU)'s Intelligent Workplace (IW) has been measured during the winter of 2006. The test has been performed using manufacture-installed instrumentation and supplementary temperature and humidity data loggers placed at various locations in the machine. The testing indicates that the operation of this wheel has reduced the heating load for ventilating the IW by 77%. Field testing performance agrees well with the lab testing data, which shows 82% heat recovery effectiveness under the same air flow settings used in field testing.

The measured data have been analyzed to establish the heat balance over the wheel and to determine the effect of wheel purge on this balance. The measured data have also been analyzed on the basis of heat transfer principles to relate the performance of the wheel to its design parameters and operating conditions. Finally, the lessons learned in field testing of a commercial enthalpy recovery wheel are presented.

INTRODUCTION

The air-to-air enthalpy recovery devices used in HVAC systems transfer heat and moisture between building exhaust air and outside air intake. They have the potential to reduce or eliminate the peak energy demand and overall energy consumption, particularly associated with high outside air flowrates and improved indoor humidity control. They fit well in current green building programs and are required by ASHRAE 90.1-2004 for systems where the design supply air is above 5000 cfm and the outside air flow is above 70% of total supply air flow[1].

Enthalpy recovery devices have different forms; a rotary enthalpy wheel is one of the prominent types in commercial applications due to its high sensible and latent heat recovery effectiveness as a result of large heat and mass transfer area.

Guidelines for the performance testing of air-to-air enthalpy recovery devices are provided in ASHRAE Standard 84-1991 Method of Testing Air-to-Air Heat Exchangers[2], where testing method, required data and calculation as well as testing equipment is specified. Built upon this ASHRAE Standard, ARI Standard 1060-2005 Performance Rating of Air-to-Air Heat Exchangers for Energy Recovery Ventilation Equipment[3] establishes the reporting requirements for equipment rating data as well as temperature and humidity conditions at which equipment tests are to be conducted. ARI Standard 1060-2005 serves as an industry standard for rating air-to-air heat/energy recovery devices.

While ASHRAE Standard 84-1991 can be applied to laboratory testing of air-to-air enthalpy exchangers, it may not be directly applicable to field testing due to financial and spatial constraints. In addition, air-to-air enthalpy exchanger performance in a field application may differ significantly from lab testing data due to the following reasons[4]:

- Heat and moisture exchange with the surroundings,
- Air leakage from/to the surroundings,
- Non-uniform inlet air conditions,
- Air carryover, crossover or leakage between different air streams.

The only way to determine the enthalpy exchanger performance in a field installation is through field testing.

Performance testing of enthalpy wheels is further complicated by the non-uniform outlet air conditions as a result of wheel rotation and, perhaps, non-uniform wheel structure. Building owners and operators are lack of clear

understanding of the wheel performance in their projects, despite the increasing deployment of enthalpy wheels.

Field testing helps increase the confidence in enthalpy wheel performance and promote the application of such devices. However, there has been limited research work done on this subject. Johnson et al.[5] reported the heat recovery performance of an enthalpy wheel installed in a printing building. Shang and Besant[6] recommended enthalpy wheel performance be calculated based on the data taken at one angular position.

This paper presents the winter testing results of an enthalpy wheel installed in the ventilation system of CMU's IW, based on manufacture-installed instrumentation and external temperature and humidity data loggers, which were placed at various locations in the machine. The measured data have been analyzed to establish the heat balance over the wheel and to determine the effect of wheel purge on this balance. The non-uniformity of inlet and outlet air conditions of the wheel and the impact of sensor locations on measured air temperature have been investigated. In addition, the measured data have also been analyzed on the basis of heat transfer principles to relate the performance of the wheel to its design parameters and operating conditions.

NOMENCLATURE

Abbreviations:

ARI	Air-Conditioning & Refrigeration Institute
ASHRAE	American Society of Heating, Refrigeration and Air-Conditioning Engineers
CMU	Carnegie Mellon University
EA	Exhaust Air
EW	Enthalpy Wheel
ESS	Energy Supply System
HVAC	Heating, Ventilating and Air Conditioning
IW	Intelligent Workplace
OA	Outside Air
PA	Process Air
RA	Return Air
RcA	Recirculation Air
SA	Supply Air

Parameters/Variables:

A	Area
Cp	Specific heat
dh	Enthalpy difference
dP	Pressure differential
\dot{m}	Mass flowrate
power	Fan power consumption
Q, q	Heat transfer
T	Temperature
w	Work done by the fan
ρ	density
ϵ	fan efficiency or wheel heat recovery effectiveness

Subscripts:

a	Air
bfan	Before supply fan
pg	Wheel purge
s	Sensible
ring	Piezo ring in the supply fan
sFan	Supply fan

EQUIPMENT AND INSTRUMENTATION

The enthalpy wheel shown in Figure 1, is an add-on module to a main ventilation unit which integrates a 3000 cfm circulation fan with 50 kW air cooled heat pump for cooling and heating as well as an active solid desiccant wheel for air dehumidification in summer and air heating in winter. The combined system was installed in the winter of 2005-2006 as part of the IW Energy Supply System (IWESS). During winter operation, the enthalpy wheel pre-heats the outside air before it is drawn into the main unit, where it, with perhaps recirculation air, is further heated by the heat pump coil. The system is highly instrumented, as indicated in Figure 2 as manufacture-installed sensors, for the purpose of control and performance monitoring.

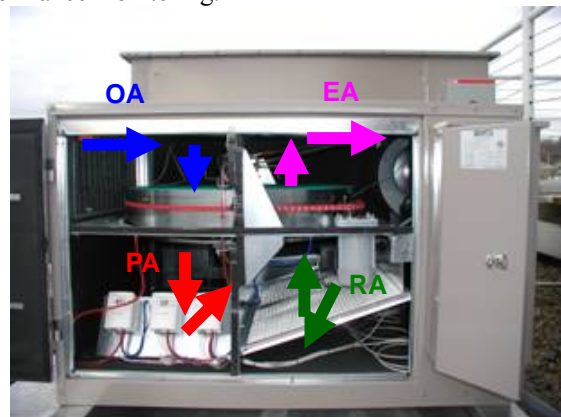


Figure 1. Enthalpy Wheel in the IW

As seen in Figure 2, temperature and relative humidity sensors are installed to measure the conditions of outside air and exhaust air from the enthalpy wheel. The return air sensors are located in the return plenum, underneath the main unit. The process air condition from the wheel is not directly measured due to spatial constraints; instead, the temperature and relative humidity of the air leaving the supply fan is recorded. Although not indicated in the diagram, pressure drops across both outside and return air sections of the enthalpy wheel are measured by pressure transducers located in the wheel assembly, which are used to calculate the process and exhaust air volumetric flowrate. Pressure change across a piezo ring in the supply fan is also measured to obtain the supply air flowrate.

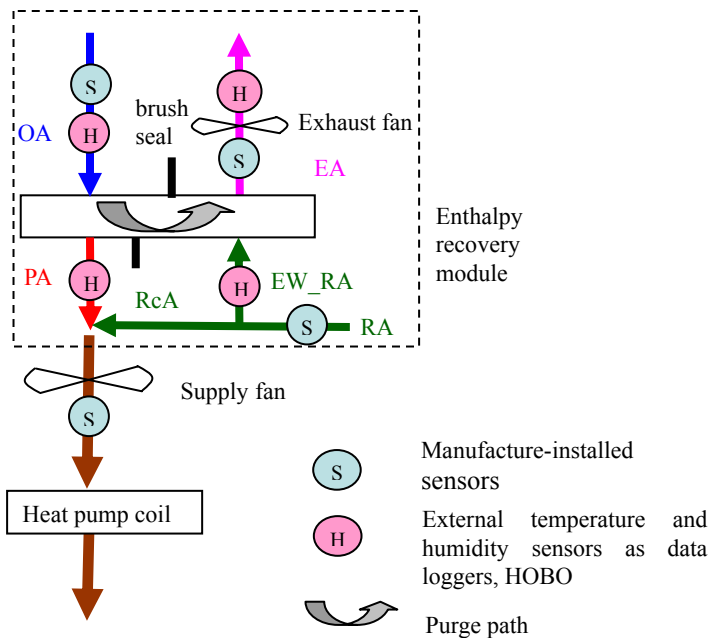


Figure 2. Schematic of the Enthalpy Wheel and Instrumentation

Due to spatial limitations, some of manufacture-installed sensors are located at places where typical representative readings of inlet and outlet air conditions may not be obtained. Therefore external temperature and humidity data loggers are deployed to explore the impact of sensor location and check the measurements obtained from manufacture-installed sensors. As shown in Figure 3, four external sensors located at different positions on a metal screen at the process air outlet from the wheel before it enters the supply fan are used to record the process air temperature and humidity. Three external sensors are used to measure the return air condition entering the enthalpy wheel. Exhaust air conditions leaving the wheel are also measured at the exhaust fan outlet where representative exhaust air condition readings can be obtained due to air mixing caused by the fan, provided that the temperature rise due to exhaust fan power consumption is reasonably accounted for. Outside air condition is also recorded using external sensor.

Only temperature and humidity data loggers are used in the experiment. The air flowrate indicated by manufacture-installed instrumentation is used in the performance calculation using both manufacture-installed and external sensors. From this aspect, the air flow is not treated as rigorously as air temperature and humidity measurement.

In order to eliminate cross-contamination between outside and building exhaust air streams, the enthalpy wheel is built with a purge section, as illustrated in Figure 4. When the wheel rotates from exhaust to outside air section, the exhaust air trapped in the channels of the wheel also gets rotated. The idea of purge is to use a small amount of outside air to remove the trapped exhaust air that will otherwise enter the process air

stream. The designed purge flowrate depends on the rotation speed and volume of the wheel.

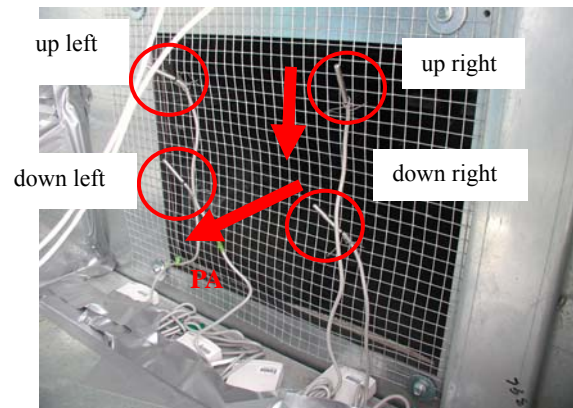


Figure 3. External Sensors Used to Measure Process Air Conditions

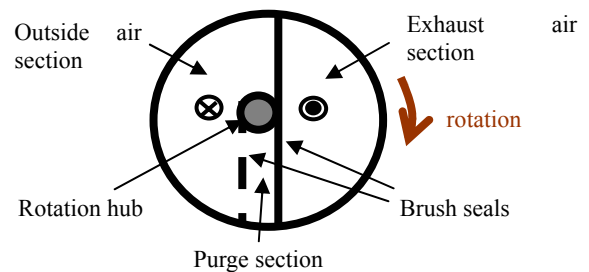


Figure 4. Top View of the Enthalpy Wheel, Indicating Wheel Purge

In the analysis of these measured data obtained in the Pittsburgh climate, the moisture exchange in the wheel is not considered due to the lack of driving potential as a result of negligible humidity difference between outside and return air streams. In essence, only sensible heat exchange performance is examined.

Specifications of the instrumentation used in this experiment are presented in Table 1.

Table 1. Instrumentation Specification

Measurement	Sensor	Accuracy
Air temperature (Manufacture-installed)	Thermistor	±0.36 °F
Air temperature (External data logger)	Thermistor	±0.20 °F
Air flow (Manufacture-installed)	Pressure transducer	±0.4% of maximum observed reading
Electric power	Current transducer	±0.5% of full scale

PERFORMANCE CALCULATION

Heat balance

With reference to Figure 2, the amount of heat gained by process air stream and heat lost by exhaust air stream is calculated as:

$$Q_{\text{gain,pa}} = \dot{m}_{\text{pa}} \cdot c_{p_a} \cdot (T_{\text{pa}} - T_{\text{oa}}) \quad (1)$$

$$Q_{\text{lost,ea}} = \dot{m}_{\text{ea}} \cdot c_{p_a} \cdot (T_{\text{ra}} - T_{\text{ea}}) \quad (2)$$

The mass flowrate of process and exhasut air streams was calculated from the outside and exhaust air pressure drop measurement across the enthalpy wheel as follows. The coefficients a, b, c and d are determined based on the testing information obtained from the wheel manufacture's lab.

$$\dot{m}_{\text{ea}} = a \cdot \rho_a \cdot dP_{\text{EWea}} \quad (3)$$

$$\dot{m}_{\text{pa}} = \rho_a \cdot \left[b \cdot \sqrt{dP_{\text{EWsa}}} - c \right]^d \quad (4)$$

where $a = 3625$, $b = 593.98$, $c = 70.93$ and $d = 1.261$

The calculation for exhaust air flowrate indicates laminar flow characteristics, which is expected given the structure of the wheel and the air flowrate. However, the calculation for process air flowrate does not indicate a pure laminar flow.

The process air temperature is calculated based on the heat balance of air mixing, which occurs before the supply fan:

$$\dot{m}_{\text{pa}} \cdot T_{\text{pa}} + \dot{m}_{\text{rca}} \cdot T_{\text{ra}} = \dot{m}_{\text{sa}} \cdot T_{\text{bfan}} \quad (5)$$

The total supply air flowrate is computed from the delta pressure measurement across the piezo ring in the supply fan. Similarly, the coefficient e is determined based on the testing information obtained from the manufacture's lab. The calculation is consistent with the flowrate measurement with a Venturi flow meter.

$$\dot{m}_{\text{sa}} = e \cdot \rho_a \cdot \sqrt{\frac{dP_{\text{sa}}}{\rho_a}} \cdot A_{\text{ring}} \quad (6)$$

where $e = 753.06$

T_{bfan} is calculated based on the air temperature leaving the supply fan and the temperature rise caused by the fan. The entire power consumption of supply fan ends up with the supply air temperature increase due to two different mechanisms: thermal energy going into the air stream due to motor and fan inefficiency; thermal effect of the air compression process in the fan.

Based on the First Law of Thermodynamics, the following equation holds for the process in the fan:

$$q = dh + w \quad (7)$$

where dh is the air enthalpy change before and after the fan, w is the work done by the fan and q is the overall heat exchange with surroundings.

Assuming the air goes through an adiabatic process in the fan, we get:

$$w = -dh \quad (8)$$

which means that the work done by the fan becomes the enthalpy increase of the processed air.

Let ϵ_{sFan} represent the total fan efficiency, which is the product of motor efficiency and blade efficiency, the work done by the supply fan can be obtained as:

$$w = \epsilon_{\text{sFan}} \cdot \text{power}_{\text{sFan}} \quad (9)$$

$$\epsilon_{\text{sFan}} \cdot \text{power}_{\text{sFan}} = \dot{m}_{\text{sa}} \cdot dT_{\text{sa,work}} \cdot c_{p_a} \quad (10)$$

On the other hand, fan inefficiency causes $(1-\epsilon_{\text{sFan}})$ portion of power consumed by the fan becomes heat entering the air stream.

$$(1 - \epsilon_{\text{sFan}}) \cdot \text{power}_{\text{sFan}} = \dot{m}_{\text{sa}} \cdot dT_{\text{sa,heat}} \cdot c_{p_a} \quad (11)$$

Overall, we have:

$$\text{power}_{\text{sFan}} = \dot{m}_{\text{sa}} \cdot dT_{\text{sa}} \cdot c_{p_a} \quad (12)$$

$$dT_{\text{sa}} = dT_{\text{sa,heat}} + dT_{\text{sa,work}} \quad (13)$$

$$T_{\text{bfan}} = T_{\text{enterdx}} - dT_{\text{sa}} \quad (14)$$

When considering purge air flow, the total heat gain will be the sum of heat gained by the process air and by the purge air stream.

$$Q_{\text{gain}} = Q_{\text{gain,pa}} + Q_{\text{gain,pg}} \quad (15)$$

where heat gained by the purge stream can be obtained from:

$$Q_{\text{gain,pg}} = \dot{m}_{\text{pg}} \cdot c_{p_a} \cdot (T_{\text{ea}} - T_{\text{oa}}) \quad (16)$$

Heat lost by the return air stream when considering purge flow becomes:

$$Q_{\text{lost,EWra}} = \dot{m}_{\text{EWra}} \cdot c_{p_a} \cdot (T_{\text{ra}} - T_{\text{ea}}) \quad (17)$$

where the return air flowrate entering the enthalpy wheel is obtained as the difference between exhaust and purge air flow since the purge flow is included in the measured exhaust air flowrate, but not in the measured process air flowrate.

$$\dot{m}_{\text{EWra}} = \dot{m}_{\text{ea}} - \dot{m}_{\text{pg}} \quad (18)$$

Heat recovery effectiveness

According to ASHRAE 84-1991, sensible heat recovery effectiveness of the wheel is defined as the ratio between actual heat transfer and the maximum possible transfer. With reference to Figure 2, the sensible heat recovery effectiveness can be calculated from heat gained by the process air and heat removed from the exhaust air as follows. The average effectiveness can be obtained by taking the arithmetic average of the two.

$$\epsilon_{\text{s,pa}} = \left[\frac{\dot{m}_{\text{pa}} \cdot (T_{\text{pa}} - T_{\text{oa}})}{\dot{m}_{\text{EWra}} \cdot (T_{\text{ra}} - T_{\text{oa}})} \right] \cdot 100 \quad (19)$$

$$\epsilon_{\text{s,ea}} = \left[\frac{\dot{m}_{\text{EWra}} \cdot (T_{\text{ra}} - T_{\text{ea}})}{\dot{m}_{\text{EWra}} \cdot (T_{\text{ra}} - T_{\text{oa}})} \right] \cdot 100 \quad (20)$$

$$\epsilon_{s,avg} = \frac{\epsilon_{s,ea} + \epsilon_{s,pa}}{2} \quad (21)$$

TESTING RESULTS AND DISCUSSION

The process and exhaust air flowrates during testing are 1300 scfm and 1080 scfm, respectively. Given a purge air flow of 80 scfm which is calculated from the wheel volume and rotary speed and confirmed by the manufacture, the resulting return air flowrate entering the wheel is 1000 scfm.

The outside (OA), return (RA), process (PA) and exhaust (EA) temperature recorded or calculated from manufacture-installed sensors is shown on the upper left plot in Figure 5. It is worthwhile mentioning that all temperature measurements shown are calibrated based on either wheel manufacture supplied information or commercial calibration devices. Assuming no purge air flow, the heat balance calculated based on this temperature history is indicated as solid squares in Figure 6. On average the heat removed from return air stream differs from the heat gained by outside air stream by 27%. Inclusion of purge air flow brings the heat gain closer to the heat loss. However, there is still a significant discrepancy between the two.

The temperature recorded by the external data loggers is shown on the upper right plot in Figure 5. Compared with the upper left plot, external data loggers indicate comparable OA temperature, lower RA temperature and higher PA and EA

temperature. As a result, the calculated heat loss is lower and calculated heat gain is higher than those obtained from manufacture-installed sensors. Figure 6 shows these data points scatter around the heat balance line within -9% ~ +3%.

The return and process air temperature shown in the upper right plot in Figure 5 indicates the arithmetic average reading from the data loggers placed at the return air inlet to and the process air outlet from the enthalpy wheel, respectively. The air velocity distribution at in the inlet and outlet of the wheel and the representative area are ignored.

As shown at the bottom of Figure 5, a T-Q plot is created to illustrate the relationship between the temperature of different air streams and the amount of heat transfer. The T-Q illustration of an enthalpy wheel is similar to that of a counter-flow heat exchanger. In an ideal enthalpy wheel which has infinite heat transfer area, process and exhaust air temperature approaches return and outside air temperature, respectively. The slope of the two lines represents the thermal mass of the two air streams.

At the instance indicated in the T-Q plot, the outside air is heated by 18.1°F; the return air is cooled by 23.9°F. The return air goes through a larger temperature change due to its smaller mass flowrate. The heat exchanged between outside and return air streams is 435.9 Btu/min. Consequently, the heating load on the subsequent heat pump coil is reduced by 435.9 Btu/min.

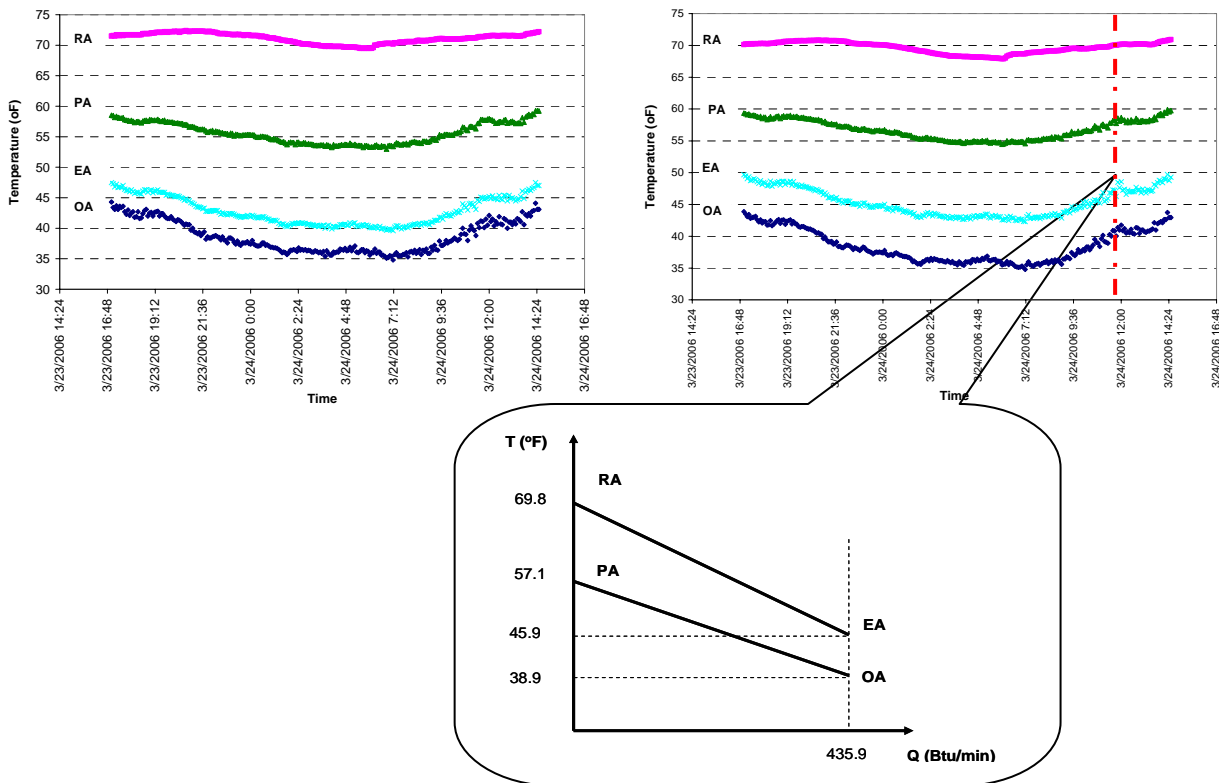


Figure 5. Enthalpy Wheel Temperature History during Testing

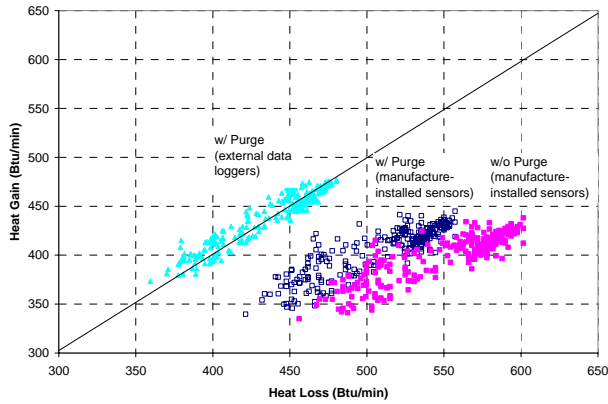


Figure 6. Enthalpy Wheel Heat Balance

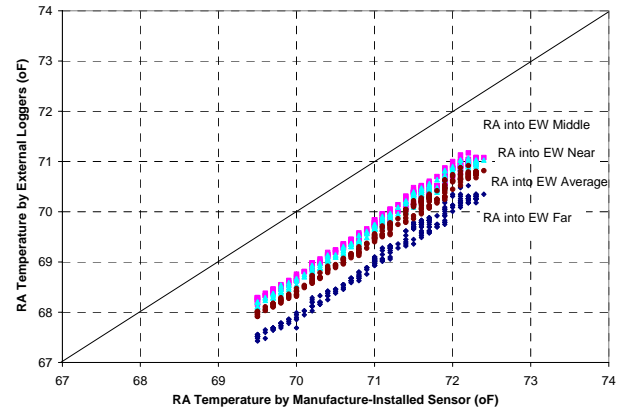


Figure 7. Return Air Temperature

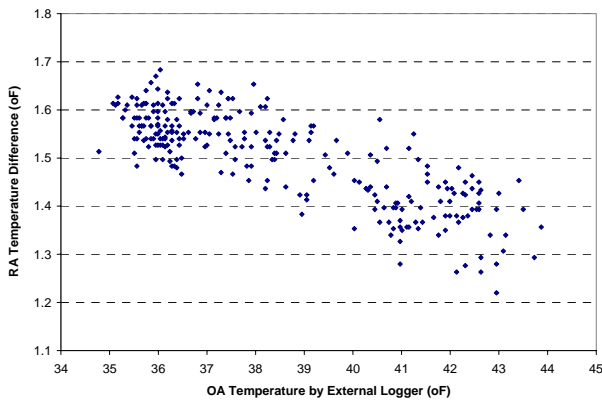


Figure 8. Return Air Temperature Difference between Manufacture-Installed Sensor and External Loggers

Figure 7 plots the readings from each individual return air temperature data logger against the return air temperature in the plenum as measured by the manufacture-installed sensor. Average return air temperature measured by the external data loggers is 1.5°F lower than that indicated by manufacture-installed sensor. It is also seen that the return air temperature entering the enthalpy wheel is spatially non-uniform. The readings from the three loggers differ from each other by 0.7°F.

Air short-circuited from the process air outlet to the return air inlet is considered as the major reason for the return air temperature discrepancy indicated by manufacture's sensor and external loggers, since the return and process air openings in the main unit is immediately adjacent to each other. This reasoning is consistent with the observation from Figure 8, which indicates the relationship between the return air temperature difference between manufacture-installed sensor and the average reading from external data loggers and the outside air conditions.

Other reasons might include air leakage from the surroundings due to the negative pressure in the chamber, air leakage around brush seals in the wheel and heat loss from the return air to the colder mixing air before the return air reaches

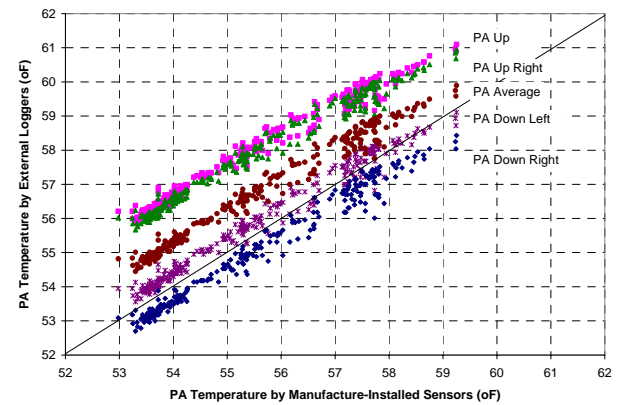


Figure 9. Process Air Temperature

the wheel. All of these factors also contribute to the non-uniform return air temperature entering the wheel.

Figure 9 plots the readings from four data loggers used to measure process air conditions. On average process air temperature calculated from manufacture-installed sensors is 1.1°F lower than that measured with external data loggers. The process air temperature difference is related to the return air temperature difference shown in Figure 10, as a result of the process air temperature calculation indicated in Equation 5. In fact, using the return air temperature readings from external data loggers to re-calculate the process air temperature based on Equation 5 reduces the discrepancy between calculated heat gain and heat loss in the wheel.

Figure 9 also shows significant temperature non-uniformity at the process air opening, which is considered as a result of spatial non-uniformity of the process air at wheel outlet and temperature stratification at the opening.

Figure 11 compares the exhaust air temperature reading from manufacture-installed sensor in the wheel assembly, the direct reading from external data logger placed after the exhaust fan and the adjusted reading to account for exhaust fan power consumption.

The exhaust fan power usage is measured as 624 W, which results in 1.8°F increase in the exhaust air temperature.

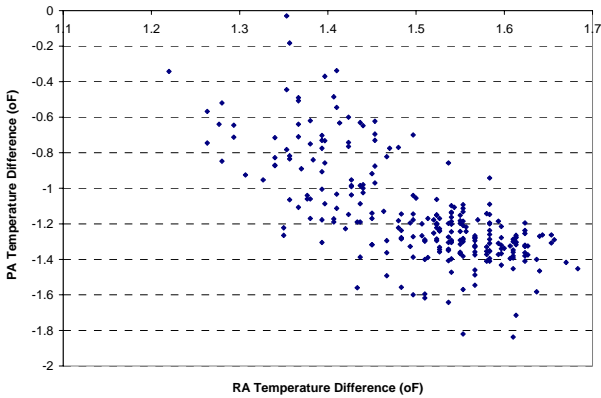


Figure 10. Process Air Temperature Difference between Manufacture-Installed Sensor and External Loggers

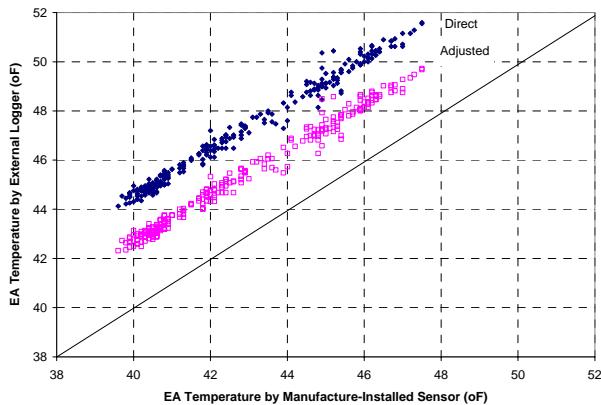


Figure 11. Exhaust Air Temperature

On average exhaust air temperature indicated by the manufacture-installed sensor is 2.5°F lower than that obtained from the external data logger even after the exhaust fan power consumption is accounted for. The major reason for this difference is the location of manufacture-installed exhaust air temperature sensor, which is believed to indicate a below-average reading since it is placed close to the separation brush seal between the outside and exhaust air chambers.

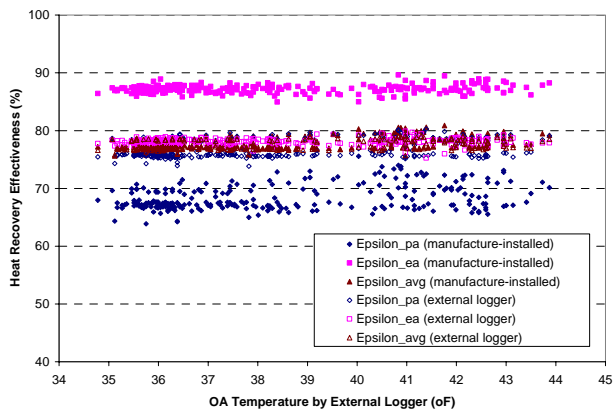


Figure 12. Sensible Heat Recovery Effectiveness

The process air side, exhaust air side and average sensible heat recovery effectiveness calculated based on readings from manufacture-installed sensors and external data loggers are plotted in Figure 12. The effectiveness is nearly constant regardless of the outside air temperature, which agrees with the results from previous research work[7,8]. The testing results indicate good heat recovery performance of the wheel; average heat recovery effectiveness is at 77%, which means 77% of the heating load required for ventilating the IW is provided through enthalpy recovery. Lab testing performance data obtained from the wheel manufacture indicates 82% sensible heat recovery effectiveness under the same air flow settings as used in field testing[9]. Field testing performance agrees well with the lab testing data, considering the complexities in field testing. Also seen from Figure 12, there is large difference between process and exhaust air side heat recovery effectiveness calculated from manufacture-installed sensor readings, which can be explained by the large discrepancy in heat balance data with such readings. On the other hand, the process and exhaust air side effectiveness calculated from external data loggers agrees with each other within $\pm 6\%$. Interestingly, the average effectiveness calculated from manufacture-installed sensors and external data loggers is almost the same, which is understood as a coincidence for this experiment. This understanding will be further reviewed in summer performance testing.

HEAT TRANSFER ANALYSIS

A finite-difference model based on fundamental scientific and engineering principles has been developed to relate the winter operating performance of the wheel to its design parameters and operating conditions. The model is able to successfully simulate the temperature distribution in the desiccant and the non-uniform outlet temperature of the process and exhaust air. The sensible heat recovery effectiveness obtained in field testing agrees well with the simulation results. Without considering the impact of non-uniform inlet air conditions, the model over-predicts heat transfer by 3%, compared with field testing results.

LESSONS LEARNED IN FIELD TESTING

Field testing is the only means to determine the operating performance of an enthalpy recovery wheel installed in an application. However, field testing is a difficult task due to the non-uniform nature of air conditions leaving the wheel as well as various heat and air exchanges within the wheel and its surroundings. Due to these factors, field performance of an enthalpy wheel is often different from lab testing results.

Obtaining representative temperature readings of the wheel inlet and outlet air streams is challenging but critical in determining the operating performance. Representative readings are easier to obtain after air mixing devices such as fans. However, the measured temperature has to be adjusted to account for the thermal effect caused by these devices. Another way to achieve representative measurement is to take

readings at multiple locations and to take averages. Since the air velocity could also be non-uniform at different sections of the wheel, a weighted average to include the effect of different air flowrates and representative areas is preferred.

The objective is to characterize the wheel performance; therefore, inlet and outlet air conditions should be measured at places as close to the wheel as possible. As seen from this study, the return air temperature in the plenum differed from the return air temperature entering the wheel by 1.5°F. In addition, as a general rule, the air conditions should be measured directly whenever possible, since calculated values have larger uncertainty than measured quantities used in the calculation.

Determining the heat balance of the wheel is critical in establishing the validity of its heat recovery effectiveness. As shown in this study, calculated effectiveness can differ by 20% when wheel heat gain is not balanced with heat loss. If the wheel is built with a purge section, heat gained by or removed from the purge airflow should be considered in heat balance calculation.

SUMMARY AND CONCLUSION

This study presents the winter testing results of an enthalpy wheel installed in the ventilation system of CMU's IW. Using the readings from manufacture-installed sensors, which are located at positions where typical representative readings may not be obtained, the heat loss and heat gain in the wheel differ from each other by 27%. Inclusion of purge air flow in the calculation improves the heat balance calculation; however there still exists significant discrepancy in heat gain and loss. By using carefully placed external temperature data loggers, the wheel heat balance is established within -9% ~ +3%.

Heat recovery effectiveness of the wheel is nearly constant regardless of the outside air temperature. The average heat recovery effectiveness during field testing is 77%, which means enthalpy recovery provides 77% of the heating load required for ventilating the IW. Field testing results agree well with lab testing data and the prediction from a detailed heat transfer model which considers the design parameters and operating conditions of the wheel.

REFERENCES

- [1] ANSI/ASHRAE Standard 90.1-2004, Energy Standard for Building Except Low-rise Residential Buildings, ASHRAE, Atlanta.
- [2] ANSI/ASHRAE Standard 84-1991, Method of Testing Air-to-Air Heat Exchangers, ASHRAE, Atlanta.
- [3] ARI Standard 1060-2005, Performance Rating of Air-to-Air Heat Exchangers for Energy Recovery Ventilation Equipment, ARI, Arlington.
- [4] ASHARE, 2000, Systems and Equipment Handbook, ASHRAE, Atlanta.
- [5] Johnson, A. B., Simonson, C. J. and Besant, R. W., 1998, Uncertainty Analysis in the Testing of Air-to-Air

Heat/Energy Exchangers Installed in Buildings, ASHRAE Transaction, 104(1).

- [6] Shang, W. and Besant, R. W., 2001, Energy Wheel Effectiveness Evaluation, Part II: Testing and Monitoring Energy Wheels in HVAC Applications, ASHRAE Transaction, 107(2).
- [7] Kays, W. M. and London, A. L., 1984, Compact Heat Exchangers, Third Edition, McGraw-Hill, New York.
- [8] Simonson, C. J., Ciepliski, D. L. and Besant, R. W., 1999, Determining the Performance of Energy Wheels: Part I- Experimental and Numerical Methods, ASHRAE Transaction, 105(1).
- [9] Downing, C. C., 1998, Independent Performance Verification of SEMCO's Total Energy Recovery Wheels, Part 2b, Test Results for FV Series of Total Energy Recovery Wheels, Report Prepared by Georgia Tech Research Institute for SEMCO Inc.